Available online at www.sciencedirect.com

ScienceDirect

Procedia CIRP 60 (2017) 20 – 25

www.elsevier.com/locate/procedia

27th CIRP Design 2017

On design and tribological behaviour of laser textured surfaces

D. Bhaduri[a,*], A. Batal[a], S.S. Dimov[a], Z. Zhang[b], H. Dong[b], M. Fallqvist[c], R. M'Saoubi[d]

[a] *Department of Mechanical Engineering, School of Engineering, University of Birmingham, Edgbaston, Birmingham, B15 2TT, UK*
[b] *School of Metallurgy and Materials, University of Birmingham, Edgbaston, Birmingham, B15 2TT, UK*
[c] *Seco Tools AB, Fagersta, SE-737 82, Sweden*
[d] *Seco Tools (UK) Ltd., Springfield Business Park, Alcester, Warwickshire, B49 6PU, UK*

* Corresponding author. Tel.: +44-121-414-4143; fax: +44-121-414-3958. *E-mail address:* debajyoti.bhaduri@gmail.com, d.bhaduri@bham.ac.uk

Abstract

The paper reports an investigation into the functional response of textured surfaces with different designs that incorporated arrays of micro-dimples and grooves (40µm diameter/width and 15µm depth for both patterns) produced on tungsten carbide (WC) blocks by employing nanosecond (ns) and femtosecond (fs) lasers. In particular, the tribological performance of the textured WC blocks against stainless steel (SS316L) counterbody was evaluated in terms of friction and wear under dry condition compared to an untextured specimen. Friction tests were carried out on a reciprocating sliding tester while unidirectional ball-on-disc method was utilised to assess wear on the mating surfaces. The untextured surface exhibited a continuous rise in the friction coefficient from 0.15 to 0.5 from the start of the cycle to the end while the specimens textured with ns and fs lasers reached steady-state condition after 100 and 200 cycles with values between 0.35-0.45 and 0.3-0.4, respectively. Energy dispersive spectroscopy following wear tests showed a pronounced material transfer from the balls to the textured surfaces with stainless steel filling up some of the dimple and groove cavities; however, the reverse phenomenon was not apparent. Additionally, texturing with the fs laser exhibited formation of nano-ripples/structures in the produced dimples and grooves that can be further studied for creating nano-textured cutting tools or surfaces with super-hydrophobic/anti-ice properties.

Peer-review under responsibility of the scientific committee of the 27th CIRP Design Conference

Keywords: Laser texturing; tribology; sliding test; friction; wear; nano-texture

1. Introduction

Surface texturing/structuring has witnessed a substantial progress over the past decades as it is seen as a viable option for surface engineering, resulting in significant improvements in load capacity, wear resistance and friction coefficient of tribo-mechanical parts [1], thereby contributing to the development of sustainable manufacturing and surface functionalisation of components. Various techniques of surface texturing have been developed over the years including additive [2] and subtractive methods such as abrasive machining [3], reactive ion etching [4], electron beam [5] and electro discharge texturing [6]. In comparison to other subtractive material processing technologies, laser surface texturing (LST) has attracted considerable interest for over ~20 years due to its superior flexibility, selectivity, accuracy, efficiency and capability for producing tailor-made surfaces with varying wettability, adhesion and friction properties. Typically LST is carried out by producing arrays of micro-dimples/pores on the surfaces that can serve either as a micro-hydrodynamic bearing in cases of full or mixed lubrication, a micro-reservoir of lubricant in boundary or starved lubrication conditions, or as a micro-trap for wear debris in either lubricated or dry sliding environment [7].

There has been a comprehensive study on the application of LST in improving the tribological performance of friction units. Etsion et al. [8] developed an analytical model to predict the relation between the opening force and operating conditions in a mechanical seal textured with spherical micropores. The area density of the pores and the radius ratio of the seal had a marginal effect on the average pressure, whereas the effect of the pores' depth over diameter ratio was very significant. A unidirectional sliding test on hardened H13 steel specimen textured with micro-dimples broadened the

Peer-review under responsibility of the scientific committee of the 27th CIRP Design Conference
doi:10.1016/j.procir.2017.02.050

range of hydrodynamic lubrication regime in terms of load and sliding speed for both high and low viscosity oil lubricants [9]. It was further recommended that the removal of bulges at the edge of the dimples by lapping after LST was essential in order to optimise the advantageous effects of LST.

Attempt has been made to optimise the LST process parameters to benefit from textured surfaces under different lubrication regimes. Vilhena et al. [10] studied the tribological performance of AISI 52100 steel (structured with various laser pulse numbers, pulse energies and single as well as multi-mode pulses), in a low frequency - long displacement reciprocating sliding test under boundary lubrication condition. The LST specimens typically exhibited a higher coefficient of friction (COF) with respect to the untextured counterpart although texturing was beneficial in reducing the COF at low sliding speeds. On contrary to [10], the positive effects of micro-dimples became apparent with an increase in dimple depth as well as for higher sliding speeds, as observed in another study by Vilhena et al. [11]. It was argued that at greater sliding speeds, micro-dimples acted as micro pressure chambers, that provided a hydrodynamic action. Podgornik and Sedlaček [12] investigated the possibility of using 3D surface parameters (kurtosis and skewness) as the design parameters for selecting the optimal LST patterns for contact surfaces operating under lubricated conditions. For textured surfaces, an increase in the kurtosis and a more negative skewness, obtained by reducing the cavity size, increasing the cavity depth and decreasing the texturing density, were found to yield a lower friction. Tribological behaviour of LST was also assessed in combination with a solid lubricant coating, typically MoS_2 [13,14] and WS_2/Zr [15] with an aim to replace the hazardous lubricating fluids used in rotating/moving mechanical parts/systems.

Laser texturing has been applied on different materials including hardened AISI 52100 [11] and stainless steel [16], cast iron [17], Ti-6Al-4V [13], tungsten carbide [14], Al_2O_3/TiC [15], Si_3N_4/TiC [18] and nickel based superalloys [19]. Ahmed et al. [20] conducted a systematic characterisation of femtosecond laser induced nano- and micro-scale surface features on titanium, stainless steel, aluminium and copper. While undulating grooves covered with ripples and lumpy structures were formed on titanium and steel, maze-like and bumpy features on aluminium and nano-forest, deep well-defined trenches and chaotic rugged microstructures on copper were observed, as shown in Fig. 1.

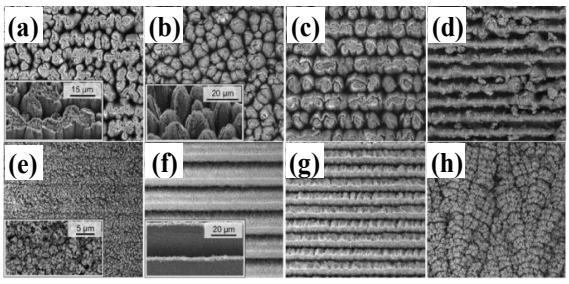

Fig. 1. Representative laser-induced surface structures observed on (a)-(d) aluminium and (f)-(h) copper [20].

Surface texturing was carried out by applying the two main laser-material interaction regimes, i.e. thermal (ns pulse durations) [10,14] and athermal (fs pulse durations) [15,19] lasers. While the former regime is dominated by thermal effects, e.g. metal melting and consequent material re-deposition and re-solidification, the latter leads to almost negligible thermal load and removes material by direct matter sublimation. Athermal processing can also result in nano-textures/ripples on surfaces that have many potential applications in the fields of biomimicry, super-hydrophobicity, colour marking for counterfeit protection and microfluidics; thus the mechanism of nano-texture formation has attracted significant research interest [20].

Although various designs and optimisation of LST patterns have been investigated, the process design methods are still dominated by 'trial and error' approaches, and yet there are large variations in 'optimum' designs obtained by different research groups [1]. The broad objectives of this research is to investigate the effectiveness of LST primarily in dry machining that have been studied by other researchers, too [21], and also to explore its potential benefits in other application areas. Dry machining with textured cutting tools has enormous prospects in sustainable design and manufacturing as it can replace the use of environmentally hazardous cutting fluids. However, it is imperative to identify the texture designs, i.e. LST patterns, and subsequently validate them in order to maximise their functional effects. The authors have investigated different LST designs, i.e. dimples and grooves with various sizes and densities created using ns laser) on tungsten carbide (WC) blocks and cutting inserts to understand the dependencies between the tribological properties and machining performance of textured tools when dry turning Ti-6Al-4V. The results of the investigation have been reported elsewhere [22,23]. Based on the knowledge gathered in [22,23], the current research presents two different designs of LST patterns (dimples and channels of equivalent dimensions but different area coverage) generated on cemented carbide surfaces using both ns and fs lasers and compares their tribological behaviour with respect to an untextured WC counterpart. As the study is ultimately aimed at assessing the machining performance of LST WC tools for dry turning a stainless steel (to be reported elsewhere), the tribology tests reported in this paper utilised SS316L ball as the counterbody. Both reciprocating and unidirectional ball-on-disc tests were carried out under dry environment to determine the friction and wear mechanisms of the textured surfaces under low and high sliding speeds.

2. Experimental details

2.1 Laser surface texturing of WC blocks

Two different laser textured patterns, comprising dimples and grooves, were produced on planar tungsten carbide blocks (20 mm×20 mm×5 mm) with nominal compositions of 94% WC and 6% Co. The trials were conducted on a Lasea L5 laser micromachining centre using both nanosecond and femtosecond lasers of wavelengths 1064 and 1030 nm and a maximum average power of 50 W and 5W, respectively. The

power, frequency, pulse width and scanning speed of the ns laser were set at 40 W, 8300 Hz, 220 ns and 1 m/s respectively while those for the fs source were 3.6 W, 500 kHz, 310 fs and 700 mm/s. These process settings were selected based on some preliminary trials. The designed dimples and grooves had diameter/width and depth of 40 and 15 µm while the textured patterns covered 10% and 32.2% of the two respective surface areas. The patterns' designs were selected based on the results obtained in [22,23] and also from one of the LST designs described in [13]. Multiple laser passes were performed until the desired pattern dimensions were achieved. An Alicona G5 InfiniteFocus microscope was utilised to measure the texture depth and diameter/width. Figure 2 depicts the LST patterns produced with ns and fs lasers.

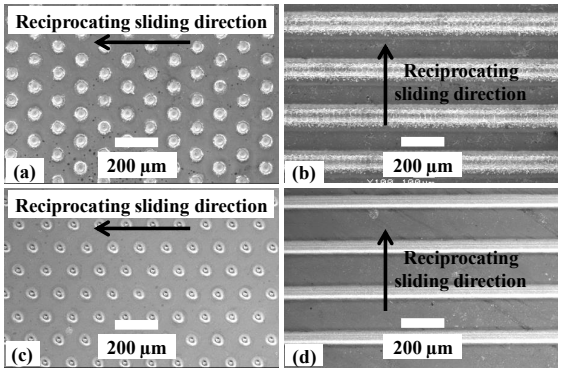

Fig. 2. Different patterns of LST: (a) dimples and (b) channels produced with ns laser, (c) dimples and (d) channels generated with fs laser source.

2.2 Tribological tests

A TE-79 reciprocating sliding tester was employed to assess the tribological behaviour of the laser textured WC surfaces in terms of friction and wear. A stainless steel (AISI 316L) ball with a diameter of 8 mm and polished to a roughness (R_a) of 0.050 µm was slid against the textured specimens under oscillating motion with a linear speed and sliding distance of 10 mm/s and 5 mm, respectively, for 1000 cycles under a static load of 20 N. The COFs were continuously recorded during the trials and compared against that of an untextured WC surface tested under equivalent conditions. All trials were carried out twice under a dry environment at atmospheric condition (22 ± 2 °C temperature and 50 ± 10% relative humidity) and the average COF was calculated.

As the reciprocating sliding tests involved a low linear speed (10 mm/s only) unidirectional ball-on-disc method was applied using the same stainless steel balls as the counterbody to evaluate the wear mechanism of the LST surfaces at a much higher velocity of 262 mm/s, i.e. ~16 m/min (10 mm mean track diameter, 500 RPM). Each trial was carried out for 38 min (a total sliding distance of 590 m) under dry condition. The parameters in ball-on-disc tests were chosen in a manner consistent with follow up SS316L turning experiments (results yet to be published). In particular, these trials involved uncoated but textured WC inserts with an expected tool life of 5 min when machining at a cutting velocity of 118 m/min that would render an equivalent sliding length of 590 m of the tool rake face under the flowing chips.

The surface condition/wear on the textured and untextured specimens and SS balls following tribology tests were analysed using a JEOL 6060 scanning electron microscope (SEM) coupled with an OXFORD INCA energy dispersive X-ray spectroscopy (EDX), whereas the roughness of the mating bodies were measured using the Alicona microscope.

3. Results and discussion

3.1 Assessment of the produced dimples and grooves

Figure 3 shows representative dimples and grooves with the achieved profiles. The diameter and depth of the dimples varied between 38-43 µm and 13-15 µm while the width and depth of the channels were within 40-43 µm and 12-15.5 µm respectively, irrespective of the laser source employed. The values suggest that the laser parameters were suitably chosen to produce textures with consistent dimensions. Enlarged views of the patterns in Fig. 4 shows microcracks and bulges (of height 5-9 µm) generated on the dimples' sidewalls produced with ns laser (Fig. 4(a)), which was the result of the applied thermal material removal mechanism. Similar LST topographies were reported in [10]. The ns laser-generated channels also exhibited re-solidified materials towards the edges together with pulse overlapping marks in the centre (Fig. 4(b)). In contrast, both dimples and grooves created using fs laser were free from re-deposited metal/edge-bulging and showed the formation nano-textures/ripples within the processed surface area, shown in Figs. 4(c) and 4(d). Similar nano-patterns were also seen when fs laser texturing of Al_2O_3/TiC ceramic [15] or C263 Ni based superalloy [19].

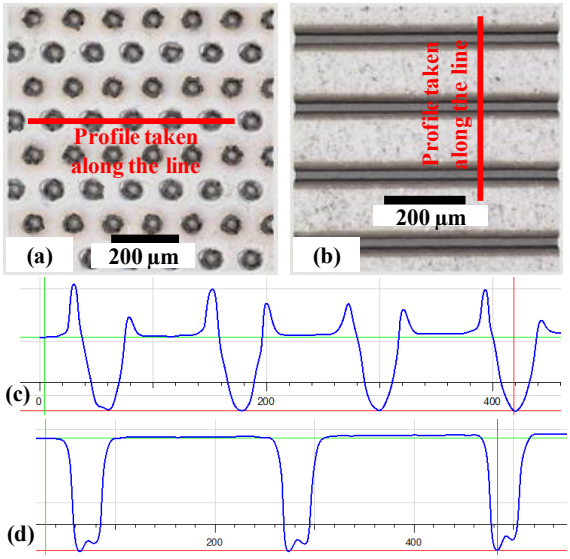

Fig. 3. Profiles of LST patterns: (a) dimples produced with ns laser and (c) their profiles, (b) channels created with fs laser and (d) their profiles.

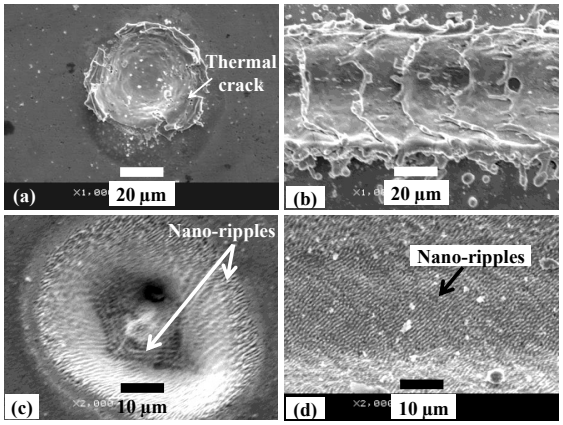

Fig. 4. Enlarged views of the LST patterns: (a) dimple and (b) channel produced using ns laser, (c) dimple and (d) channel generated using fs laser.

3.2 Reciprocating sliding tests

The static COF of the textured and untextured WC specimens recorded during the reciprocating sliding tests against SS316L balls are presented in Fig. 5. Although the initial COF of the untextured surface was lower than those of the textured ones, it steadily increased from 0.15 at the beginning of the cycle to ~0.5 towards the end of the test. In contrast, the specimens textured with ns and fs lasers reached steady-state condition after 100 and 200 cycles (i.e. 1 and 2 m of sliding distance) with COF between 0.35-0.45 and 0.3-0.4, respectively. These values were much lower than those reported by Borghi et al. [24] (COF=0.75-0.85) when dry tribology tests of textured nitriding steel against AISI 52100 counterbody.

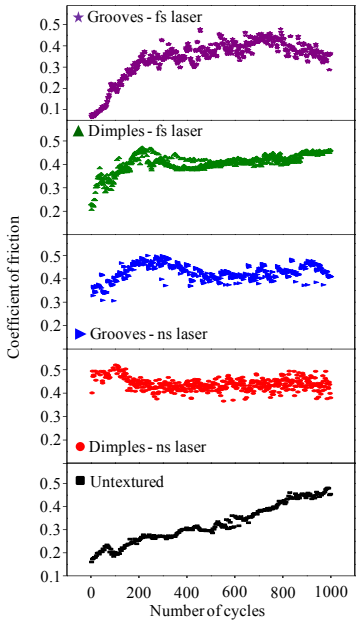

Fig. 5. Coefficient of friction vs. number of cycles for all textured and untextured specimens.

The SEM micrographs of the ns laser-produced dimples and channels showed localised material transfer from the SS ball to the textured surfaces, with only some of the dimples and grooves partially filled with steel, as shown in Fig. 6(a) and 6(b). This was supported by a spot EDX analysis carried out on one of the transferred layers where the elements of stainless steel were detected. The surface was also partially oxidised as evident from the presence of oxygen (2.59 wt%) in the elemental compositions.

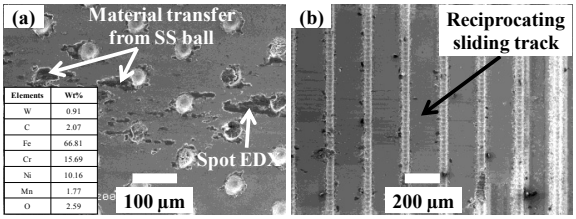

Fig. 6. SEM images of (a) dimples and (b) grooves produced using ns laser.

Figure 7(a) displays SEM of the sliding track on the carbide surface textured with fs laser-produced dimples that were partly filled with SS counterbody material. An enlarged view of a dimple in Fig. 7(b) reveals the wear debris inside the micropore and the corresponding EDX data confirms the presence of Fe, Cr and Ni as the major constituting elements together with an affirmation of marginal surface oxidation (3.34 wt% of oxygen).

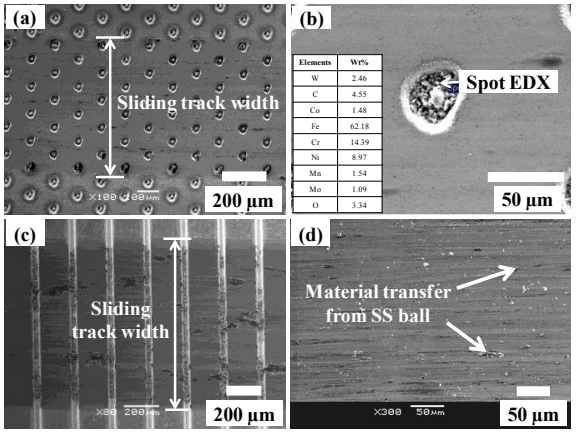

Fig. 7. SEM micrographs of (a) dimples produced using fs laser together with the sliding track width shown, (b) an enlarged dimple with the location of spot EDX, (c) SEM of sliding track on the channels created using fs laser, (d) untextured WC surface after reciprocating sliding.

Similar to Fig. 6(b) the sliding track on the channels created with fs laser also showed localised patches of transfer layer, partially filling some of the grooves, see Fig. 7(c). Both surfaces in Fig. 7(a) and 7(c) showed minimal signs of abrasion marks which were, in contrast, prevalent on the untextured WC surface subject to reciprocating sliding (Fig. 7(d)). This was possibly the reason for the increasing trend of untextured specimen's COF throughout the sliding test. Conversely, the dimples and channels acted as traps for wear

debris that reduced the extent of abrasion and supported the load during sliding [25], while the transfer layer formed on the textured samples served as a third body between the mating surfaces that stabilised the friction coefficient.

3.3 Unidirectional ball-on-disc tests

The wear tracks generated on all textured surfaces in ball-on-disc test and their magnified images are shown in Fig. 8 and Fig. 9 respectively. The degree of the transfer layer formation was greater in unidirectional sliding as much higher sliding velocity (~16 m/s) was employed in this test compared to reciprocating motion (10 mm/s). The majority of dimples and channels in the centre of the wear tracks were filled with counterbody material as the softer SS ball rubbed over much harder WC surface. It is evident from the high magnification images that the SS material first covered the micropores and channels and then smeared over the surfaces in certain regions along the sliding direction as the junction between the mating bodies transformed from non-conformal to conformal contact. The rest of the areas between dimples and channels were marginally covered with tightly adhered material although loosely worn steel particles together with some abrasion marks can be seen in Fig. 9. An EDX area mapping on the worn textured WC surface in Fig. 10 exhibits the presence of W and Co along with Fe, Cr and O in the trapped and loose wear debris.

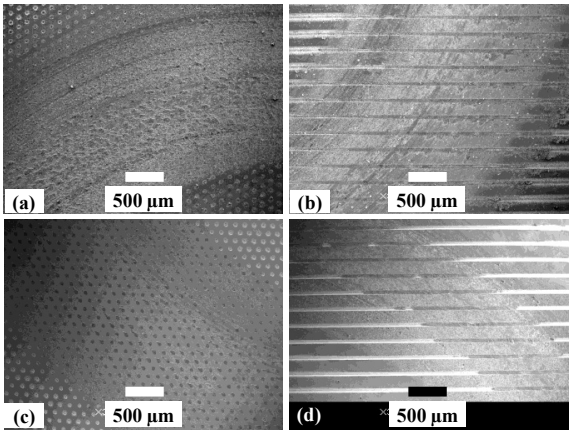

Fig. 8. Wear tracks generated on (a) dimples and (b) channels produced using ns laser, and on (c) dimples and (d) channels produced using fs laser.

Figures 11(a) and 11(b) show the wear scars on SS balls that rubbed against dimple textured and untextured WC blocks respectively. Although the wear scars on balls sliding against textured samples were larger than that of the ball sliding against smooth surfaces (as also reported in [26]), EDX analysis showed that there was negligible material transfer from the LST carbide surface to the SS counterbody. The formation of the stainless steel transfer layer and wear debris was possibly responsible for this phenomenon. Conversely, fractured WC particles were detected on the ball's worn area rubbed on the untextured WC specimen (Fig. 11(c)), which is also evident from the corresponding EDX spectra (Fig. 11(d)). This resulted in an 80% higher surface roughness on the ball's worn surface in the latter case (S_a=1.24 µm) compared to those measured on the wear scars (S_a=0.49-67µm) produced on textured samples.

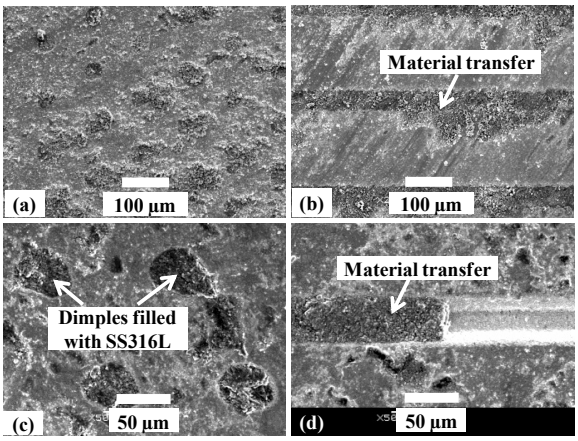

Fig. 9. Formation of transfer layers on (a) dimples and (b) channels produced using ns laser, (c) dimples and (d) channels produced using fs laser.

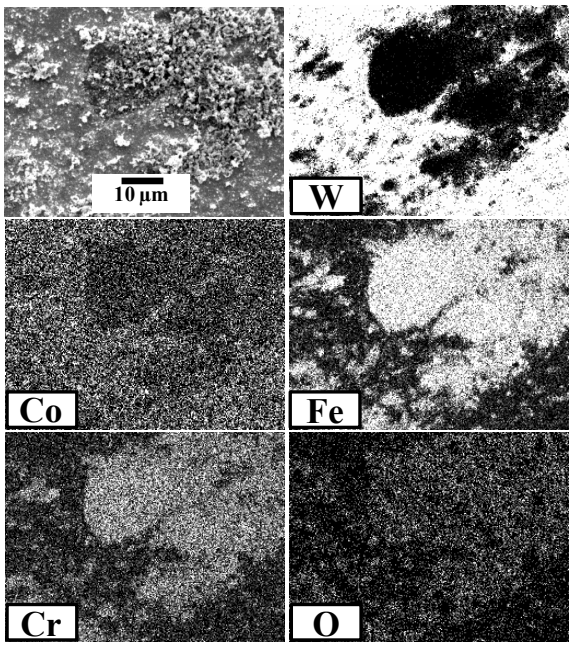

Fig. 10. EDX area mapping on a worn textured WC surface showing the presence of oxidised steel material in the trapped and loose wear debris.

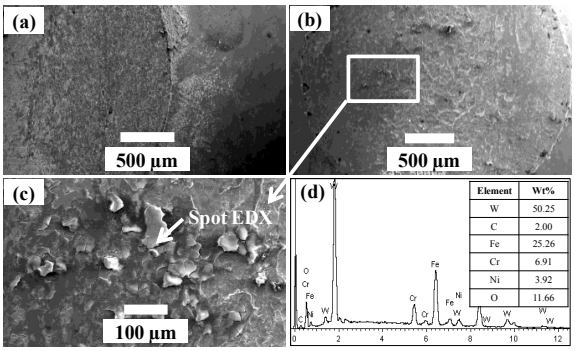

Fig. 11. Wear scars on the balls slid against (a) ns dimple textured and (b) untextured WC surfaces, (c) enlarged view of the wear scar shown in (b), (d) its corresponding EDX spectra showing adhered WC particles on SS ball.

4. Conclusions

Stainless steel transfer layers were observed on all of the textured WC specimens, while some of the dimples/grooves were partly filled with SS debris. The micropores/channels acted as traps of worn particles while the transfer layer served as an intermediate third body between the mating surfaces that stabilised the COF (between 0.35 to 0.45) in low speed reciprocating sliding tests. The extent of material transfer from the SS ball to the patterned WC specimens increased in unidirectional tests involving higher sliding velocity, while that from the carbide surface to the steel body was not apparent. On the contrary, COF of the smooth WC surface increased steadily from 0.15 to 0.5 in reciprocating sliding trials together with the transfer of materials between the mating bodies in both directions. The wear track on the untextured sample also showed numerous abrasion marks. The results indicate that there is a substantial scope for the applications of LST in sustainable manufacturing, such as machining under dry or near dry/minimum quantity lubrication (MQL) conditions where textured cutting tools are expected to stabilise/minimise the chip-tool interface friction and reduce the tool wear while the re-deposited materials at the periphery of the dimples/channels can act as micro-chip breakers. Additionally, the formation of nano-ripples in the textures produced with fs laser also has significant potential for its use in the fields of biomedical, MEMS, microfluidics and super-hydrophobicity.

Acknowledgements

The research was supported by the H2020 MAESTRO and Laser4Fun projects (Grant Agreement No. 723826 and 675063).

References

[1] Etsion I. State of the art in laser surface texturing. J Tribol, ASME Trans 2005;127:248-53.
[2] Bruzzone AAG, Costa HL, Lonardo PM, Lucca DA. Advances in engineered surfaces for functional performance. CIRP Ann, Manuf Technol 2008;57:750-69.
[3] Saka N, Tian H, Suh NP. Boundary lubrication of undulated metal surfaces at elevated temperatures. Tribol Trans 1989;32(3):389-95.
[4] Wang X, Kato K, Adachi K. The lubrication effect of micro-pits on parallel sliding faces of SiC in water. Tribol Trans 2002;45(3):294-301.
[5] Pawelski O, Rasp W, Zwick W, Nettelbeck H-J, Steinhoff K. The influence of different work-roll texturing systems on the development of surface structure in the temper rolling process of steel sheet used in the automotive industry. J Mater Proc Technol 1994;45: 215-22.
[6] Aspinwall DK, Wise MLH, Stout KJ, Goh THA, Zhao FL, El-Menshawy MF. Electrical discharge texturing. Int J Mach Tools Manuf 1992;32:183-93.
[7] Etsion I. Improving tribological performance of mechanical seals by laser surface texturing. Proceedings 17th Int Pump Users Sympos 2000; 17-21.
[8] Etsion I, Kligerman Y, Halperin G. Analytical and experimental investigation of laser-textured mechanical seal faces. Tribol Trans 1999;42(3):511-6.
[9] Kovalchenko A, Ajayi O, Erdemir A, Fenske G, Etsion I. The effect of laser surface texturing on transitions in lubrication regimes during unidirectional sliding contact. Tribol Int 2005;38:219-25.
[10] Vilhena LM, Sedlaček M, Podgornik B, Vižintin J, Babnik A, Možina J. Surface texturing by pulsed Nd:YAG laser. Tribol Int 2009;42:1496-1504.
[11] Vilhena LM, Podgornik B, Vižintin J, Možina J. Influence of texturing parameters and contact conditions on tribological behaviour of laser textured surfaces. Meccanica 2011;46:567-75.
[12] Podgornik B, Sedlaček M. Performance, characterization and design of textured surfaces. J. Tribol 2012;134:041701-1-7.
[13] Ripoll MR, Simič R, Brenner J, Podgornik B. Friction and lifetime of laser surface-textured and MoS_2-coated Ti6Al4V under dry reciprocating sliding. Tribol Lett 2013;51:261-71.
[14] Wu Z, Deng J, Xing Y, Cheng H, Zhao J. Effect of surface texturing on friction properties of WC/Co cemented carbide. Mater Des 2012;41:142-9.
[15] Xing Y, Deng J, Zhou Y, Li S. Fabrication and tribological properties of Al_2O_3/TiC ceramic with nano-textures and WS_2/Zr soft-coatings. Surf Coat Technol 2014;258:699-710.
[16] Hu J, Xu H. Friction and wear behaviour analysis of the stainless steel surface fabricated by laser texturing under water. Tribol Int 2016;102:371-7.
[17] Kim B, Chae YH, Choi HS. Effects of surface texturing on the frictional behaviour of cast iron surfaces. Tribol Int 2014;70:128-35.
[18] Xing Y, Deng J, Wu Z, Cheng H. Effect of regular surface textures generated by laser on tribological behavior of Si_3N_4/TiC ceramic. Appl Surf Sci 2013; 265:823-832.
[19] Semaltianos NG, Perrie W, French P, Sharp M, Dearden G, Watkins KG. Femtosecond laser surface texturing of a nickel-based superalloy. Appl Surf Sci 2008;255:2796-802.
[20] Ahmmed KMT, Ling EJY, Servio P, Kietzig A-M. Introducing a new optimization tool for femtosecond laser-induced surface texturing on titanium, stainless steel, aluminium and copper. Opt Laser Eng 2015;66:258-68.
[21] Kümmel J, Braun D, Gibmeier J, Schneider J, Greiner C, Schulze V, Wanner A. Study on micro texturing of uncoated cemented carbide cutting tools for wear improvement and built-up edge stabilisation. J Mater Proc Technol 2015;215:62-70.
[22] Bhaduri D, Batal A, Fallqvist M, Dimov SS, Soo SL, M'Saoubi R. The effects of laser surface texturing on scratch test and machining performance of tungsten carbide tools when turning Ti-6Al-4V. 11th Int Conf Micro Manuf, ICOMM, Irvine, USA 2016.
[23] Bhaduri D, Batal A, Fallqvist M, Dimov SS, Soo SL, M'Saoubi R. Laser texturing of tungsten carbide tools: the effects on tribological performance when machining Ti-6Al-4V alloy. Euspen's 16th Int Conf, Nottingham, UK 2016.
[24] Borghi A, Gualtieri E, Marchetto D, Moretti L, Valeri S. Tribological effects of surface texturing on nitriding steel for high-performance engine applications. Wear 2008;265:1046-51.
[25] Yamakiri H, Sasaki S, Kurita T, Kasashima N. Effects of laser surface texturing on friction behavior of silicon nitride under lubrication with water. Tribo Int 2011;44:579-84.
[26] Xing Y, Deng J, Feng X, Yu S. Effect of laser surface texturing on Si_3N_4/TiC ceramic sliding against steel under dry friction. Mater Des 2013;52:234-45.